Accelerating PDE-Constrained Optimization using Adaptive Reduced-Order Models: Application to Topology Optimization

Matthew J. Zahr

Farhat Research Group
Stanford University

Robert J. Melosh Medal Competition, Duke University
April 24, 2015

Overview

Finite Element Analysis

Model Reduction

Reduced Topology Optimization

Topology Optimization

Optimization Theory

Overview

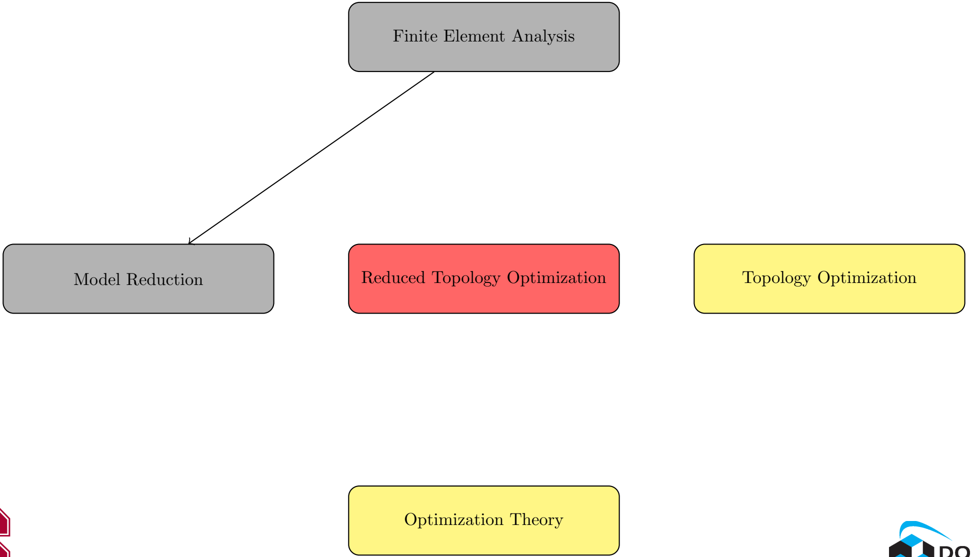
Finite Element Analysis
Model Reduction
Reduced Topology Optimization
Topology Optimization
Optimization Theory

Overview

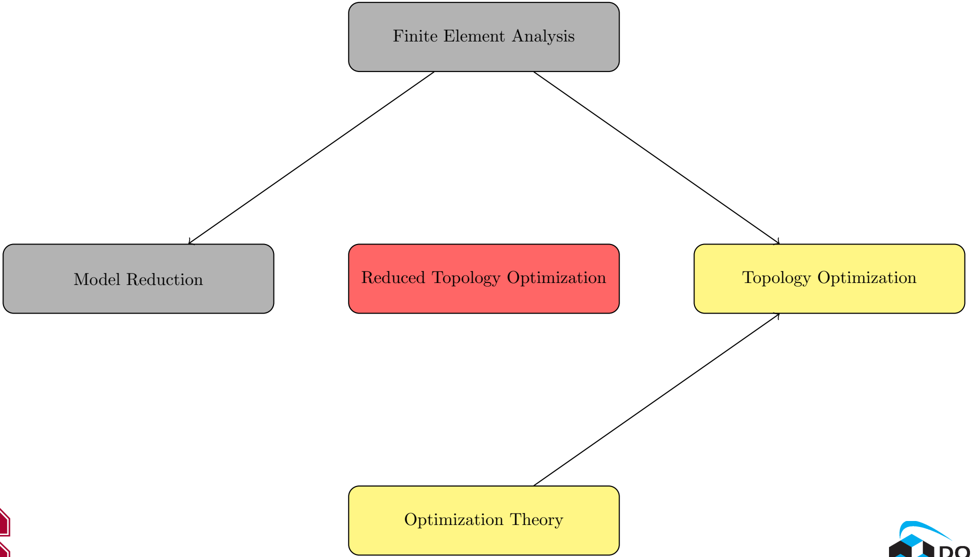
Finite Element Analysis
Model Reduction
Reduced Topology Optimization
Topology Optimization
Optimization Theory

Overview

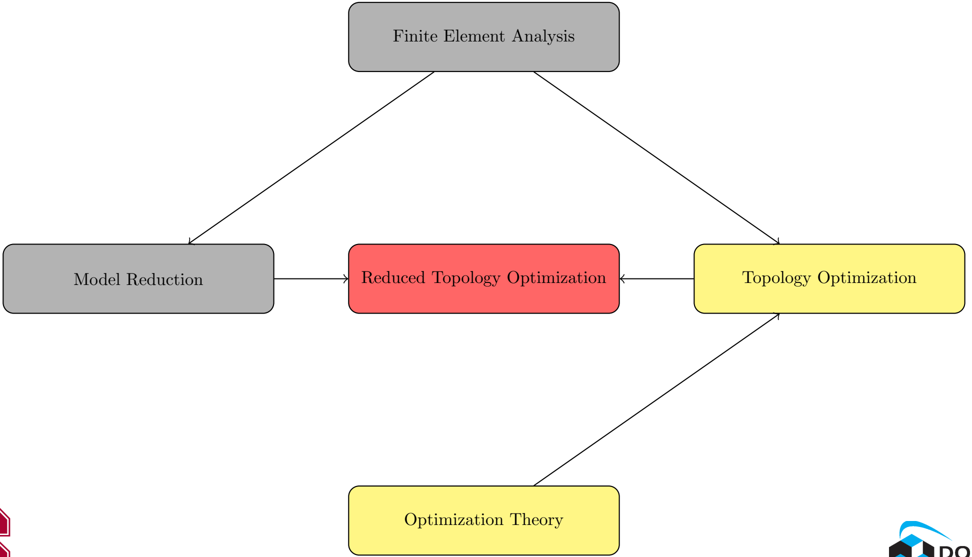
Finite Element Analysis
Model Reduction
Reduced Topology Optimization
Topology Optimization
Optimization Theory

Overview

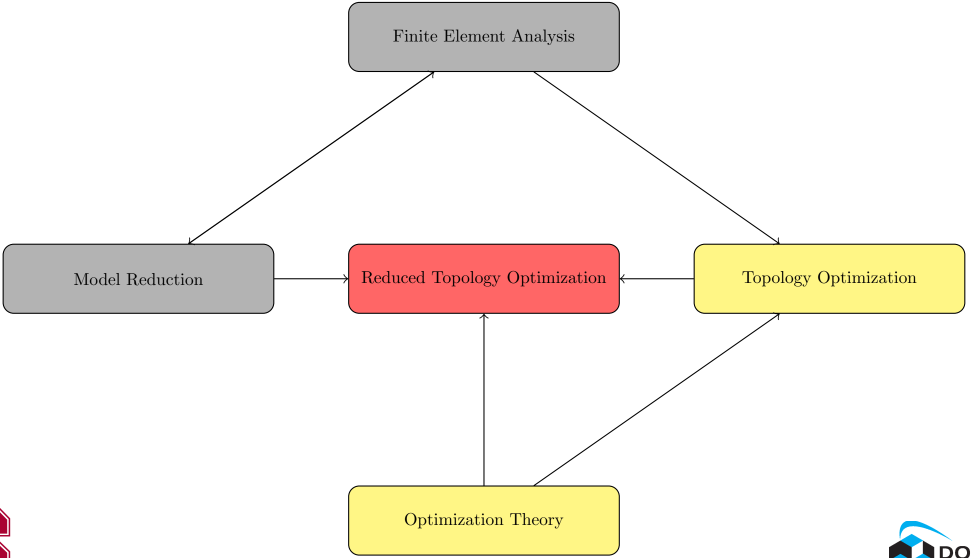
Finite Element Analysis
Model Reduction
Reduced Topology Optimization
Topology Optimization
Optimization Theory

Overview

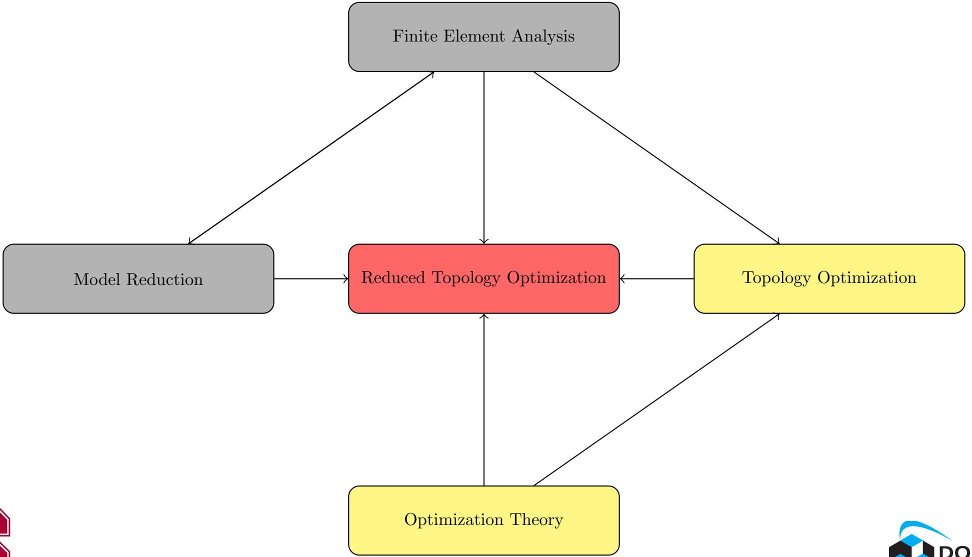
Finite Element Analysis
Model Reduction
Reduced Topology Optimization
Topology Optimization
Optimization Theory

Problem Formulation

Goal: Rapidly solve PDE-constrained optimization problem of the form

$$\begin{aligned} \underset{\mathbf{u}\in\mathbb{R}^{n_{\mathbf{u}}},\ \boldsymbol{\mu}\in\mathbb{R}^{n_{\boldsymbol{\mu}}}}{\text{minimize}} \quad & \mathcal{J}(\mathbf{u},\ \boldsymbol{\mu}) \\ \text{subject to} \quad & \mathbf{c}(\mathbf{u},\ \boldsymbol{\mu}) \geq 0 \\ & \mathbf{r}(\mathbf{u},\ \boldsymbol{\mu}) = 0 \\ & \mathbf{A}\boldsymbol{\mu} \geq \mathbf{b} \end{aligned}$$

where

- $\mathbf{r} : \mathbb{R}^{n_{\mathbf{u}}} \times \mathbb{R}^{n_{\boldsymbol{\mu}}} \rightarrow \mathbb{R}^{n_{\mathbf{u}}}$ is the discretized (steady, nonlinear) PDE
- $\mathcal{J} : \mathbb{R}^{n_{\mathbf{u}}} \times \mathbb{R}^{n_{\boldsymbol{\mu}}} \rightarrow \mathbb{R}$ is the objective function
- $\mathbf{c} : \mathbb{R}^{n_{\mathbf{u}}} \times \mathbb{R}^{n_{\boldsymbol{\mu}}} \rightarrow \mathbb{R}^{n_{\mathbf{c}}}$ are the side constraints
- $\mathbf{A} \in \mathbb{R}^{n_{\mathbf{A}} \times n_{\boldsymbol{\mu}}}$, $\mathbf{b} \in \mathbb{R}^{n_{\mathbf{A}}}$ are linear constraints (independent of $\mathbf{u}$)
- $\mathbf{u} \in \mathbb{R}^{n_{\mathbf{u}}}$ is the PDE state vector
- $\boldsymbol{\mu} \in \mathbb{R}^{n_{\boldsymbol{\mu}}}$ is the vector of parameters
- *red indicates a large quantity (i.e. scales with size of FE mesh)*
- *blue indicates a small quantity (i.e. size independent of size of FE mesh)*

Problem Setup

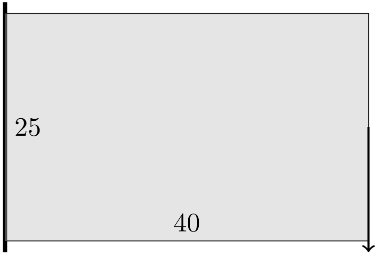

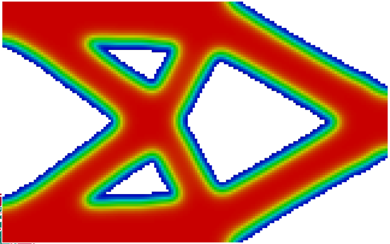

- 16000 8-node brick elements, 77760 dofs
- Total Lagrangian form, finite strain, StVK [1]
- St. Venant-Kirchhoff material
- Sparse Cholesky linear solver (CHOLMOD[2])
- Newton-Raphson nonlinear solver
- Minimum compliance optimization problem

$$\begin{aligned} \underset{\mathbf{u}\in\mathbb{R}^{n_{\mathbf{u}}},\ \boldsymbol{\mu}\in\mathbb{R}^{n_{\boldsymbol{\mu}}}}{\text{minimize}} \quad & \mathbf{f}_{\text{ext}}{}^T\mathbf{u} \\ \text{subject to} \quad & V(\boldsymbol{\mu}) \leq \frac{1}{2}V_0 \\ & \mathbf{r}(\mathbf{u},\ \boldsymbol{\mu}) = 0 \end{aligned}$$

- Gradient computations: Adjoint method
- Optimizer: SNOPT [Gill et al., 2002]

[1] [Bonet and Wood, 1997, Belytschko et al., 2000]
[2] [Chen et al., 2008]

Projection-Based Model Reduction

- Model Order Reduction (MOR) assumption: *state vector lies in low-dimensional subspace*

$$\mathbf{u} \approx \mathbf{\Phi_u} \mathbf{u}_r$$

  where
  - $\mathbf{\Phi_u} = \begin{bmatrix} \phi_{\mathbf{u}}^1 & \cdots & \phi_{\mathbf{u}}^{k_{\mathbf{u}}} \end{bmatrix} \in \mathbb{R}^{n_{\mathbf{u}} \times k_{\mathbf{u}}}$ is the reduced basis
  - $\mathbf{u}_r \in \mathbb{R}^{k_{\mathbf{u}}}$ are the reduced coordinates of $\mathbf{u}$
  - $n_{\mathbf{u}} \gg k_{\mathbf{u}}$
- Substitute assumption into High-Dimensional Model (HDM), $\mathbf{r}(\mathbf{u}, \ \boldsymbol{\mu}) = 0$, and apply Galerkin projection

$$\hat{\mathbf{r}}_r(\mathbf{u}_r, \ \boldsymbol{\mu}) = \mathbf{\Phi_u}^T \mathbf{r}(\mathbf{\Phi_u} \mathbf{u}_r, \ \boldsymbol{\mu}) = 0$$

Connection to Finite Element Method

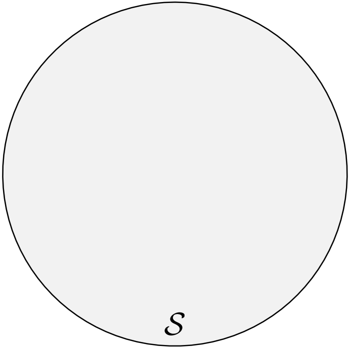

- $\mathcal{S}$ - infinite-dimensional trial space

Connection to Finite Element Method

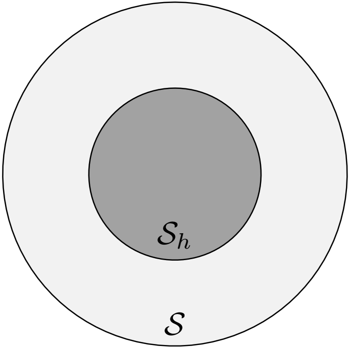

- $\mathcal{S}$ - infinite-dimensional trial space
- $\mathcal{S}_h$ - (large) finite-dimensional trial space

Connection to Finite Element Method

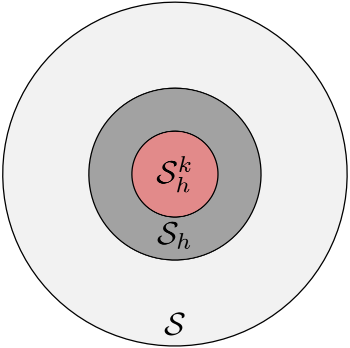

- $\mathcal{S}$ - infinite-dimensional trial space
- $\mathcal{S}_h$ - (large) finite-dimensional trial space
- $\mathcal{S}_h^k$ - (small) finite-dimensional trial space
- $\mathcal{S}_h^k \subset \mathcal{S}_h \subset \mathcal{S}$

Reduced Basis Construction

Method of Snapshots [Sirovich, 1987]

- Collect state snapshots by sampling parameter space: $\mathbf{u}(\boldsymbol{\mu})$

$$\mathbf{X} = \begin{bmatrix} \mathbf{u}(\boldsymbol{\mu}_1) & \cdots & \mathbf{u}(\boldsymbol{\mu}_n) \end{bmatrix}$$

Proper Orthogonal Decomposition (POD) [Sirovich, 1987, Holmes et al., 1998]

- Compress snapshot matrix using POD, or truncated Singular Value Decomposition (SVD)

$$\Phi_{\mathbf{u}} = \text{POD}(\mathbf{X})$$

- Trial subspace selection
  - Finite element method: polynomial basis; local support
  - Rayleigh-Ritz: analytical, empirical basis functions; global support
  - POD: data-driven, empirical basis functions; global support

Restriction of Parameter Space

- Parameter restriction: *restrict parameter to a low-dimensional subspace*

$$\boldsymbol{\mu} \approx \boldsymbol{\Phi}_{\boldsymbol{\mu}} \boldsymbol{\mu}_r$$

  - $\boldsymbol{\Phi}_{\boldsymbol{\mu}} = \begin{bmatrix} \boldsymbol{\phi}_{\boldsymbol{\mu}}^1 & \cdots & \boldsymbol{\phi}_{\boldsymbol{\mu}}^{k_{\boldsymbol{\mu}}} \end{bmatrix} \in \mathbb{R}^{n_{\boldsymbol{\mu}} \times k_{\boldsymbol{\mu}}}$ is the reduced basis
  - $\boldsymbol{\mu}_r \in \mathbb{R}^{k_{\boldsymbol{\mu}}}$ are the reduced coordinates of $\boldsymbol{\mu}$
  - $n_{\boldsymbol{\mu}} \gg k_{\boldsymbol{\mu}}$
- Substitute restriction into Reduced-Order Model, $\hat{\mathbf{r}}_r(\mathbf{u}_r,\ \boldsymbol{\mu}) = 0$ to obtain

$$\mathbf{r}_r(\mathbf{u}_r,\ \boldsymbol{\mu}_r) = \boldsymbol{\Phi}_{\mathbf{u}}{}^T \mathbf{r}(\boldsymbol{\Phi}_{\mathbf{u}} \mathbf{u}_r,\ \boldsymbol{\Phi}_{\boldsymbol{\mu}} \boldsymbol{\mu}_r) = 0$$

- Related work:
  [Maute and Ramm, 1995, Lieberman et al., 2010, Constantine et al., 2014]

Restriction of Parameter Space

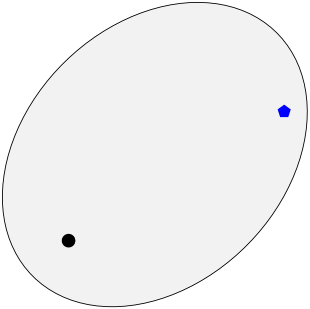

Parameter space

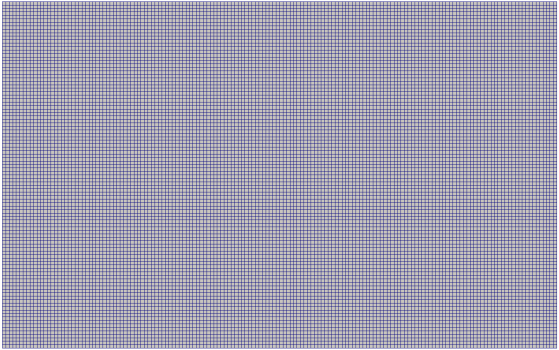

Cantilever mesh

Restriction of Parameter Space

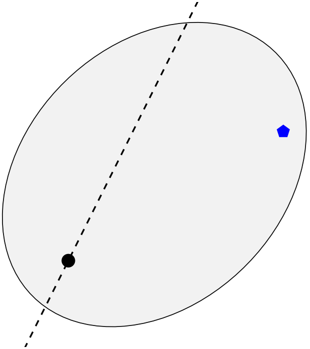

Parameter space

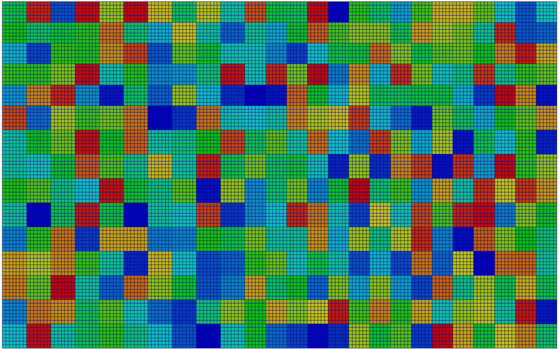

Macroelements

Standard Difficulty: Binary Solutions

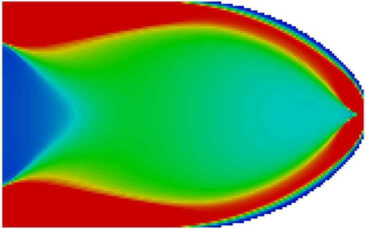

(a) Without penalization

Standard Difficulty: Binary Solutions

Relaxed, Penalized Problem Setup

$$\begin{aligned} \underset{\mathbf{u}\in\mathbb{R}^{n_{\mathbf{u}}},\ \boldsymbol{\mu}\in\mathbb{R}^{n_{\boldsymbol{\mu}}}}{\text{minimize}} \quad & \mathbf{f}_{\text{ext}}{}^T\mathbf{u} \\ \text{subject to} \quad & V(\boldsymbol{\mu}) \leq \frac{1}{2}V_0 \\ & \mathbf{r}(\mathbf{u},\ \boldsymbol{\mu}^p) = 0 \\ & \boldsymbol{\mu} \in [0,1]^{k_{\boldsymbol{\mu}}} \end{aligned}$$

Effect of Penalization

$$\mathbf{K}^e \leftarrow (\boldsymbol{\mu}^e)^p\mathbf{K}^e$$

- $\mathbf{K}^e$: eth element stiffness matrix

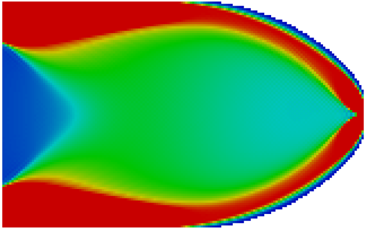

(a) Without penalization

Standard Difficulty: Binary Solutions

Relaxed, Penalized Problem Setup

$$\begin{aligned} \underset{\mathbf{u}\in\mathbb{R}^{n_{\mathbf{u}}},\ \boldsymbol{\mu}\in\mathbb{R}^{n_{\boldsymbol{\mu}}}}{\text{minimize}} \quad & \mathbf{f}_{\text{ext}}{}^T\mathbf{u} \\ \text{subject to} \quad & V(\boldsymbol{\mu}) \leq \frac{1}{2}V_0 \\ & \mathbf{r}(\mathbf{u},\ \boldsymbol{\mu}^p) = 0 \\ & \boldsymbol{\mu} \in [0,1]^{k_{\boldsymbol{\mu}}} \end{aligned}$$

Effect of Penalization

$$\mathbf{K}^e \leftarrow (\boldsymbol{\mu}^e)^p\mathbf{K}^e$$

- $\mathbf{K}^e$: eth element stiffness matrix

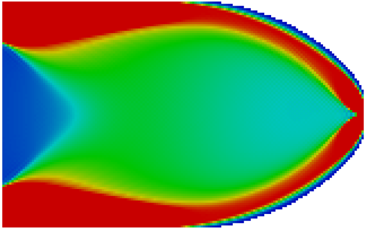

(a) Without penalization

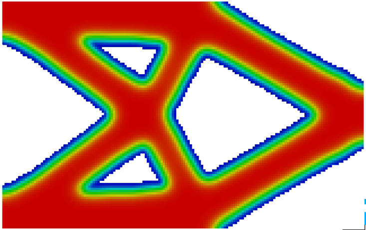

(b) With penalization

Standard Difficulty: Binary Solutions

Implication for ROM

- From parameter restriction, $\boldsymbol{\mu}^p = (\boldsymbol{\Phi}_\mu \boldsymbol{\mu}_r)^p$
- Precomputation relies on separability of $\boldsymbol{\Phi}_\mu$ and $\boldsymbol{\mu}_r$
- Separability maintained if $(\boldsymbol{\Phi}_\mu \boldsymbol{\mu}_r)^p = \boldsymbol{\Phi}_\mu \boldsymbol{\mu}_r{}^p$
- Sufficient condition: *columns of* $\boldsymbol{\Phi}_\mu$ *have non-overlapping non-zeros*

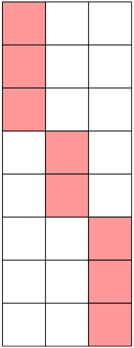

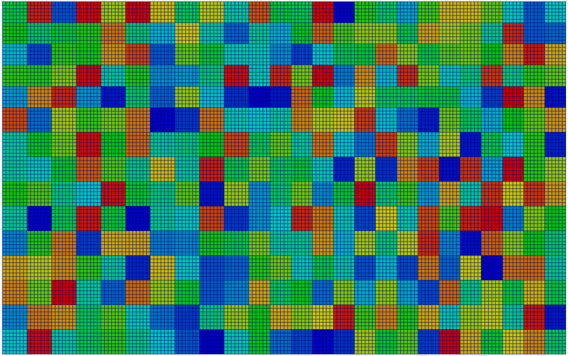

Reduced Optimization Problem

$$
\begin{aligned}
\underset{\mathbf{u}_r \in \mathbb{R}^{k_{\mathbf{u}}},\ \boldsymbol{\mu}_r \in \mathbb{R}^{k_{\boldsymbol{\mu}}}}{\text{minimize}} \quad & \mathcal{J}(\boldsymbol{\Phi}_{\mathbf{u}}\mathbf{u}_r,\ \boldsymbol{\Phi}_{\boldsymbol{\mu}}\boldsymbol{\mu}_r) \\
\text{subject to} \quad & \mathbf{c}(\boldsymbol{\Phi}_{\mathbf{u}}\mathbf{u}_r,\ \boldsymbol{\Phi}_{\boldsymbol{\mu}}\boldsymbol{\mu}_r) \geq 0 \\
& \mathbf{r}(\boldsymbol{\Phi}_{\mathbf{u}}\mathbf{u}_r,\ \boldsymbol{\Phi}_{\boldsymbol{\mu}}\boldsymbol{\mu}_r) = 0 \\
& \boldsymbol{\Phi}_{\boldsymbol{\mu}}^T \mathbf{A} \boldsymbol{\Phi}_{\boldsymbol{\mu}}\boldsymbol{\mu}_r \geq \boldsymbol{\Phi}_{\boldsymbol{\mu}}^T \mathbf{b}
\end{aligned}
$$

Adaptation of $\boldsymbol{\Phi}_{\mathbf{u}}$

- Control accuracy of ROM
- Trust region approach

Adaptation of $\boldsymbol{\Phi}_{\boldsymbol{\mu}}$

- Control restriction of parameter space

State-Adaptive Approach to ROM Optimization

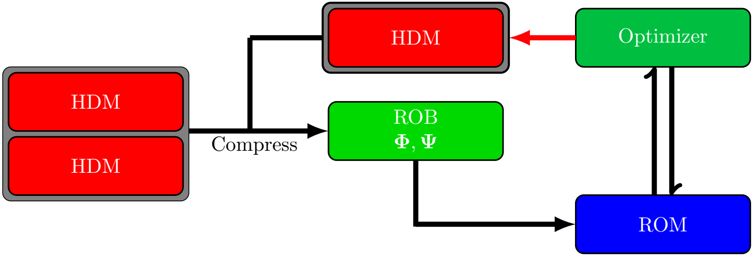

Figure: Schematic of Adaptive for ROM Optimization

Trust-Region POD

Trust-Region POD (TRPOD) [Arian et al., 2000]

$$
\begin{aligned}
\underset{\mathbf{u}_r \in \mathbb{R}^{k_{\mathbf{u}}},\ \boldsymbol{\mu}_r \in \mathbb{R}^{k_{\boldsymbol{\mu}}}}{\text{minimize}} \quad & \mathcal{J}(\boldsymbol{\Phi}_{\mathbf{u}}\mathbf{u}_r,\ \boldsymbol{\Phi}_{\boldsymbol{\mu}}\boldsymbol{\mu}_r) \\
\text{subject to} \quad & \mathbf{c}(\boldsymbol{\Phi}_{\mathbf{u}}\mathbf{u}_r,\ \boldsymbol{\Phi}_{\boldsymbol{\mu}}\boldsymbol{\mu}_r) \geq 0 \\
& \mathbf{r}(\boldsymbol{\Phi}_{\mathbf{u}}\mathbf{u}_r,\ \boldsymbol{\Phi}_{\boldsymbol{\mu}}\boldsymbol{\mu}_r) = 0 \\
& {\boldsymbol{\Phi}_{\boldsymbol{\mu}}}^T \mathbf{A} \boldsymbol{\Phi}_{\boldsymbol{\mu}}\boldsymbol{\mu}_r \geq {\boldsymbol{\Phi}_{\boldsymbol{\mu}}}^T \mathbf{b} \\
& ||\boldsymbol{\mu}_r - \bar{\boldsymbol{\mu}}_r|| \leq \Delta
\end{aligned}
$$

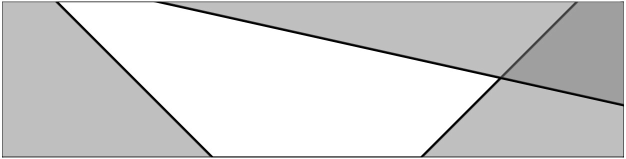

Trust-Region POD

Trust-Region POD (TRPOD) [Arian et al., 2000]

$$
\begin{aligned}
\underset{\mathbf{u}_r \in \mathbb{R}^{k_{\mathbf{u}}},\ \boldsymbol{\mu}_r \in \mathbb{R}^{k_{\boldsymbol{\mu}}}}{\text{minimize}} \quad & \mathcal{J}(\boldsymbol{\Phi}_{\mathbf{u}}\mathbf{u}_r,\ \boldsymbol{\Phi}_{\boldsymbol{\mu}}\boldsymbol{\mu}_r) \\
\text{subject to} \quad & \mathbf{c}(\boldsymbol{\Phi}_{\mathbf{u}}\mathbf{u}_r,\ \boldsymbol{\Phi}_{\boldsymbol{\mu}}\boldsymbol{\mu}_r) \geq 0 \\
& \mathbf{r}(\boldsymbol{\Phi}_{\mathbf{u}}\mathbf{u}_r,\ \boldsymbol{\Phi}_{\boldsymbol{\mu}}\boldsymbol{\mu}_r) = 0 \\
& \boldsymbol{\Phi}_{\boldsymbol{\mu}}{}^T \mathbf{A} \boldsymbol{\Phi}_{\boldsymbol{\mu}} \boldsymbol{\mu}_r \geq \boldsymbol{\Phi}_{\boldsymbol{\mu}}{}^T \mathbf{b} \\
& ||\boldsymbol{\mu}_r - \bar{\boldsymbol{\mu}}_r|| \leq \Delta
\end{aligned}
$$

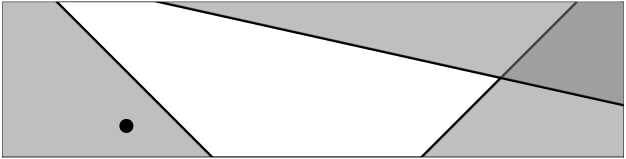

Trust-Region POD

Trust-Region POD (TRPOD) [Arian et al., 2000]

$$
\begin{aligned}
\underset{\mathbf{u}_r \in \mathbb{R}^{k_{\mathbf{u}}},\ \boldsymbol{\mu}_r \in \mathbb{R}^{k_{\mu}}}{\text{minimize}} \quad & \mathcal{J}(\boldsymbol{\Phi}_{\mathbf{u}}\mathbf{u}_r,\ \boldsymbol{\Phi}_{\mu}\boldsymbol{\mu}_r) \\
\text{subject to} \quad & \mathbf{c}(\boldsymbol{\Phi}_{\mathbf{u}}\mathbf{u}_r,\ \boldsymbol{\Phi}_{\mu}\boldsymbol{\mu}_r) \geq 0 \\
& \mathbf{r}(\boldsymbol{\Phi}_{\mathbf{u}}\mathbf{u}_r,\ \boldsymbol{\Phi}_{\mu}\boldsymbol{\mu}_r) = 0 \\
& {\boldsymbol{\Phi}_{\mu}}^T \mathbf{A} \boldsymbol{\Phi}_{\mu}\boldsymbol{\mu}_r \geq {\boldsymbol{\Phi}_{\mu}}^T \mathbf{b} \\
& ||\boldsymbol{\mu}_r - \bar{\boldsymbol{\mu}}_r|| \leq \Delta
\end{aligned}
$$

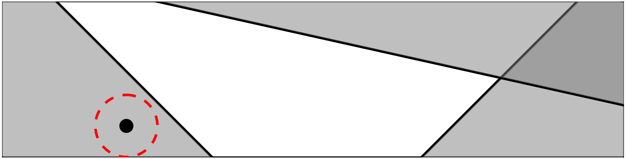

Constrained Trust-Region POD

Constrained Trust-Region POD

$$\begin{aligned}
\underset{\mathbf{u}_r\in\mathbb{R}^{k_{\mathbf{u}}},\ \boldsymbol{\mu}_r\in\mathbb{R}^{k_{\boldsymbol{\mu}}},\ \mathbf{t}\in\mathbb{R}^{n_{\mathbf{c}}}}{\text{minimize}} \quad & \mathcal{J}(\boldsymbol{\Phi}_{\mathbf{u}}\mathbf{u}_r,\ \boldsymbol{\Phi}_{\boldsymbol{\mu}}\boldsymbol{\mu}_r) - \gamma\mathbf{t}^T\mathbf{1} \\
\text{subject to} \quad & \mathbf{c}(\boldsymbol{\Phi}_{\mathbf{u}}\mathbf{u}_r,\ \boldsymbol{\Phi}_{\boldsymbol{\mu}}\boldsymbol{\mu}_r) \geq \mathbf{t} \\
& \mathbf{r}(\boldsymbol{\Phi}_{\mathbf{u}}\mathbf{u}_r,\ \boldsymbol{\Phi}_{\boldsymbol{\mu}}\boldsymbol{\mu}_r) = 0 \\
& {\boldsymbol{\Phi}_{\boldsymbol{\mu}}}^T\mathbf{A}\boldsymbol{\Phi}_{\boldsymbol{\mu}}\boldsymbol{\mu}_r \geq {\boldsymbol{\Phi}_{\boldsymbol{\mu}}}^T\mathbf{b} \\
& ||\boldsymbol{\mu}_r - \bar{\boldsymbol{\mu}}_r|| \leq \Delta \\
& \mathbf{t} \leq 0
\end{aligned}$$

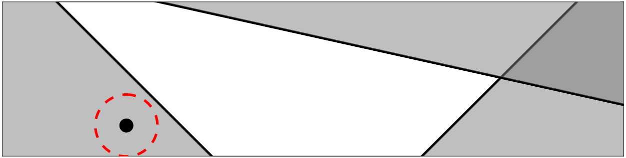

Constrained Trust-Region POD

Constrained Trust-Region POD

$$
\begin{aligned}
\underset{\mathbf{u}_r \in \mathbb{R}^{k_{\mathbf{u}}},\ \boldsymbol{\mu}_r \in \mathbb{R}^{k_{\boldsymbol{\mu}}},\ \mathbf{t} \in \mathbb{R}^{n_{\mathbf{c}}}}{\text{minimize}} \quad & \mathcal{J}(\boldsymbol{\Phi}_{\mathbf{u}}\mathbf{u}_r,\ \boldsymbol{\Phi}_{\boldsymbol{\mu}}\boldsymbol{\mu}_r) - \gamma \mathbf{t}^T \mathbf{1} \\
\text{subject to} \quad & \mathbf{c}(\boldsymbol{\Phi}_{\mathbf{u}}\mathbf{u}_r,\ \boldsymbol{\Phi}_{\boldsymbol{\mu}}\boldsymbol{\mu}_r) \geq \mathbf{t} \\
& \mathbf{r}(\boldsymbol{\Phi}_{\mathbf{u}}\mathbf{u}_r,\ \boldsymbol{\Phi}_{\boldsymbol{\mu}}\boldsymbol{\mu}_r) = 0 \\
& \boldsymbol{\Phi}_{\boldsymbol{\mu}}{}^T \mathbf{A} \boldsymbol{\Phi}_{\boldsymbol{\mu}}\boldsymbol{\mu}_r \geq \boldsymbol{\Phi}_{\boldsymbol{\mu}}{}^T \mathbf{b} \\
& ||\boldsymbol{\mu}_r - \bar{\boldsymbol{\mu}}_r|| \leq \Delta \\
& \mathbf{t} \leq 0
\end{aligned}
$$

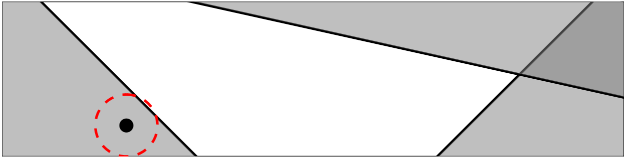

Constrained Trust-Region POD

Constrained Trust-Region POD

$$\begin{aligned}
\underset{\mathbf{u}_r \in \mathbb{R}^{k_{\mathbf{u}}},\ \boldsymbol{\mu}_r \in \mathbb{R}^{k_{\boldsymbol{\mu}}},\ \mathbf{t} \in \mathbb{R}^{n_{\mathbf{c}}}}{\text{minimize}} \quad & \mathcal{J}(\boldsymbol{\Phi}_{\mathbf{u}}\mathbf{u}_r,\ \boldsymbol{\Phi}_{\boldsymbol{\mu}}\boldsymbol{\mu}_r) - \gamma \mathbf{t}^T \mathbf{1} \\
\text{subject to} \quad & \mathbf{c}(\boldsymbol{\Phi}_{\mathbf{u}}\mathbf{u}_r,\ \boldsymbol{\Phi}_{\boldsymbol{\mu}}\boldsymbol{\mu}_r) \geq \mathbf{t} \\
& \mathbf{r}(\boldsymbol{\Phi}_{\mathbf{u}}\mathbf{u}_r,\ \boldsymbol{\Phi}_{\boldsymbol{\mu}}\boldsymbol{\mu}_r) = 0 \\
& \boldsymbol{\Phi}_{\boldsymbol{\mu}}^T \mathbf{A} \boldsymbol{\Phi}_{\boldsymbol{\mu}}\boldsymbol{\mu}_r \geq \boldsymbol{\Phi}_{\boldsymbol{\mu}}^T \mathbf{b} \\
& ||\boldsymbol{\mu}_r - \bar{\boldsymbol{\mu}}_r|| \leq \Delta \\
& \mathbf{t} \leq 0
\end{aligned}$$

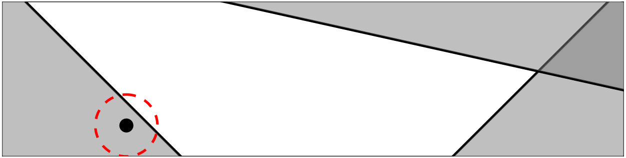

Constrained Trust-Region POD

Constrained Trust-Region POD

$$
\begin{aligned}
\underset{\mathbf{u}_r \in \mathbb{R}^{k_{\mathbf{u}}},\ \boldsymbol{\mu}_r \in \mathbb{R}^{k_{\boldsymbol{\mu}}},\ \mathbf{t} \in \mathbb{R}^{n_{\mathbf{c}}}}{\text{minimize}} \quad & \mathcal{J}(\boldsymbol{\Phi}_{\mathbf{u}}\mathbf{u}_r,\ \boldsymbol{\Phi}_{\boldsymbol{\mu}}\boldsymbol{\mu}_r) - \gamma \mathbf{t}^T \mathbf{1} \\
\text{subject to} \quad & \mathbf{c}(\boldsymbol{\Phi}_{\mathbf{u}}\mathbf{u}_r,\ \boldsymbol{\Phi}_{\boldsymbol{\mu}}\boldsymbol{\mu}_r) \geq \mathbf{t} \\
& \mathbf{r}(\boldsymbol{\Phi}_{\mathbf{u}}\mathbf{u}_r,\ \boldsymbol{\Phi}_{\boldsymbol{\mu}}\boldsymbol{\mu}_r) = 0 \\
& \boldsymbol{\Phi}_{\boldsymbol{\mu}}^T \mathbf{A} \boldsymbol{\Phi}_{\boldsymbol{\mu}}\boldsymbol{\mu}_r \geq \boldsymbol{\Phi}_{\boldsymbol{\mu}}^T \mathbf{b} \\
& ||\boldsymbol{\mu}_r - \bar{\boldsymbol{\mu}}_r|| \leq \Delta \\
& \mathbf{t} \leq 0
\end{aligned}
$$

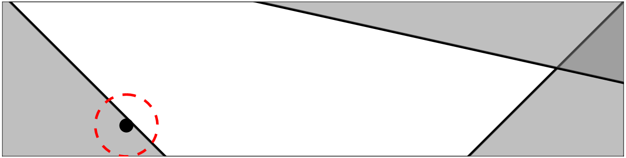

Constrained Trust-Region POD

Constrained Trust-Region POD

$$
\begin{aligned}
\underset{\mathbf{u}_r \in \mathbb{R}^{k_{\mathbf{u}}},\ \boldsymbol{\mu}_r \in \mathbb{R}^{k_{\boldsymbol{\mu}}},\ \mathbf{t} \in \mathbb{R}^{n_{\mathbf{c}}}}{\text{minimize}} \quad & \mathcal{J}(\mathbf{\Phi}_{\mathbf{u}}\mathbf{u}_r,\ \mathbf{\Phi}_{\boldsymbol{\mu}}\boldsymbol{\mu}_r) - \gamma \mathbf{t}^T \mathbf{1} \\
\text{subject to} \quad & \mathbf{c}(\mathbf{\Phi}_{\mathbf{u}}\mathbf{u}_r,\ \mathbf{\Phi}_{\boldsymbol{\mu}}\boldsymbol{\mu}_r) \geq \mathbf{t} \\
& \mathbf{r}(\mathbf{\Phi}_{\mathbf{u}}\mathbf{u}_r,\ \mathbf{\Phi}_{\boldsymbol{\mu}}\boldsymbol{\mu}_r) = 0 \\
& \mathbf{\Phi}_{\boldsymbol{\mu}}{}^T \mathbf{A} \mathbf{\Phi}_{\boldsymbol{\mu}}\boldsymbol{\mu}_r \geq \mathbf{\Phi}_{\boldsymbol{\mu}}{}^T \mathbf{b} \\
& ||\boldsymbol{\mu}_r - \bar{\boldsymbol{\mu}}_r|| \leq \Delta \\
& \mathbf{t} \leq 0
\end{aligned}
$$

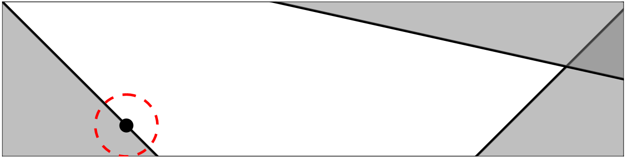

Reduced Optimization Problem

$$
\begin{aligned}
\underset{\mathbf{u}_r \in \mathbb{R}^{k_{\mathbf{u}}},\ \boldsymbol{\mu}_r \in \mathbb{R}^{k_{\boldsymbol{\mu}}}}{\text{minimize}} \quad & \mathcal{J}(\boldsymbol{\Phi}_{\mathbf{u}}\mathbf{u}_r,\ \boldsymbol{\Phi}_{\boldsymbol{\mu}}\boldsymbol{\mu}_r) \\
\text{subject to} \quad & \mathbf{c}(\boldsymbol{\Phi}_{\mathbf{u}}\mathbf{u}_r,\ \boldsymbol{\Phi}_{\boldsymbol{\mu}}\boldsymbol{\mu}_r) \geq 0 \\
& \mathbf{r}(\boldsymbol{\Phi}_{\mathbf{u}}\mathbf{u}_r,\ \boldsymbol{\Phi}_{\boldsymbol{\mu}}\boldsymbol{\mu}_r) = 0 \\
& \boldsymbol{\Phi}_{\boldsymbol{\mu}}^T \mathbf{A} \boldsymbol{\Phi}_{\boldsymbol{\mu}}\boldsymbol{\mu}_r \geq \boldsymbol{\Phi}_{\boldsymbol{\mu}}^T \mathbf{b}
\end{aligned}
$$

Adaptation of $\boldsymbol{\Phi}_{\mathbf{u}}$

- Control accuracy of ROM
- Trust region approach

Adaptation of $\boldsymbol{\Phi}_{\boldsymbol{\mu}}$

- Control restriction of parameter space

Reduced Order Basis Adaptivity: Φ_μ

- Selection of Φ_μ amounts to a *restriction* of the parameter space

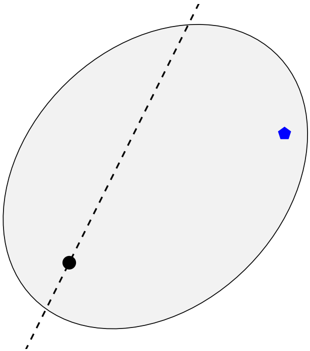

Reduced Order Basis Adaptivity: Φ_μ

- Selection of Φ_μ amounts to a *restriction* of the parameter space
- Adaptation of Φ_μ should attempt to include the optimal solution in the restricted parameter space, i.e. $\mu^* \in \text{col}(\Phi_\mu)$

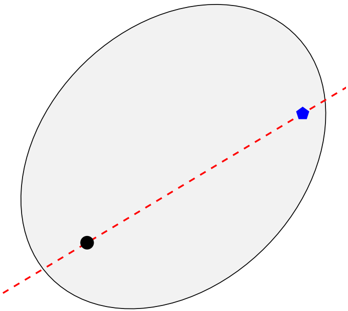

Reduced Order Basis Adaptivity: Φ_μ

- Selection of Φ_μ amounts to a *restriction* of the parameter space
- Adaptation of Φ_μ should attempt to include the optimal solution in the restricted parameter space, i.e. $\mu^* \in \text{col}(\Phi_\mu)$
- Adaptation based on **first-order optimality conditions** of HDM optimization problem

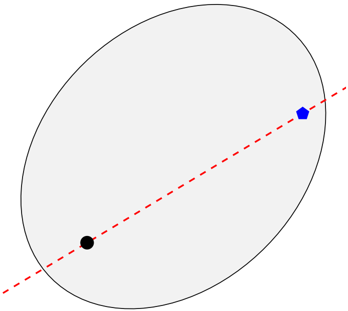

Reduced Order Basis Adaptivity: Φ_μ

Lagrangian

$$\mathcal{L}(\boldsymbol{\mu}, \boldsymbol{\lambda}, \boldsymbol{\tau}) = \mathcal{J}(\mathbf{u}(\boldsymbol{\mu}), \boldsymbol{\mu}) - \boldsymbol{\lambda}^T \mathbf{c}(\mathbf{u}(\boldsymbol{\mu}), \boldsymbol{\mu}) - \boldsymbol{\tau}^T (\mathbf{A}\boldsymbol{\mu} - \mathbf{b})$$

Karush-Kuhn Tucker (KKT) Conditions [3]

$$\begin{aligned}
\nabla_{\boldsymbol{\mu}} \mathcal{L}(\boldsymbol{\mu}, \boldsymbol{\lambda}, \boldsymbol{\tau}) &= 0 \\
\boldsymbol{\lambda} &\geq 0 \\
\boldsymbol{\tau} &\geq 0 \\
\boldsymbol{\lambda}_i \mathbf{c}_i(\mathbf{u}(\boldsymbol{\mu}), \boldsymbol{\mu}) &= 0 \\
\boldsymbol{\tau}_j (\mathbf{A}\boldsymbol{\mu} - \mathbf{b}) &= 0 \\
\mathbf{c}(\mathbf{u}(\boldsymbol{\mu}), \boldsymbol{\mu}) &\geq 0 \\
\mathbf{A}\boldsymbol{\mu} &\geq \mathbf{b}
\end{aligned}$$

- Relies heavily on **Lagrange multipliers estimates** [Zahr, 2015]

[3] [Nocedal and Wright, 2006]

Refinement Indicator

- From Lagrange multiplier estimates, only KKT condition not satisfied automatically:

$$\nabla_{\mu}\mathcal{L}(\mu,\ \lambda,\ \tau) = 0$$

- Use $|\nabla_{\mu}\mathcal{L}(\mu,\ \lambda,\ \tau)|$ as indicator for **refinement** of discretization of μ-space

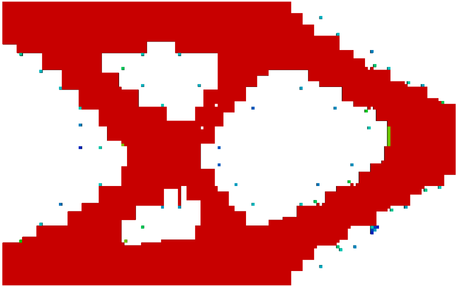

μ

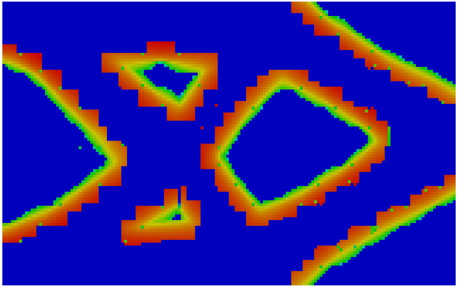

$|\nabla_{\mu}\mathcal{L}(\mu,\ \lambda,\ \tau)|$

Refinement Indicator

- From Lagrange multiplier estimates, only KKT condition not satisfied automatically:

$$\nabla_{\mu}\mathcal{L}(\mu,\ \lambda,\ \tau) = 0$$

- Use $|\nabla_{\mu}\mathcal{L}(\mu,\ \lambda,\ \tau)|$ as indicator for **refinement** of discretization of μ-space

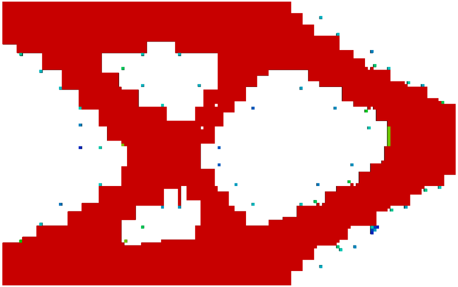

μ

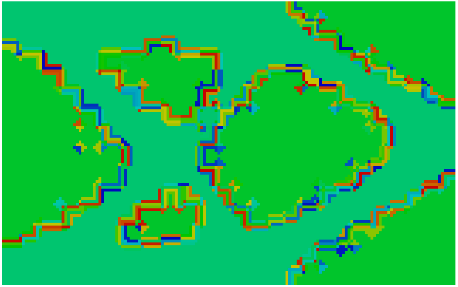

Updated Macroelements

Problem Setup

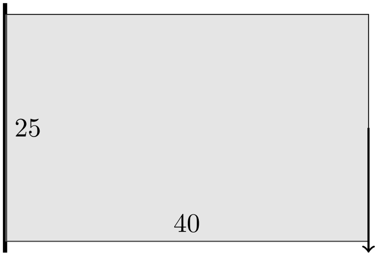

- 16000 8-node brick elements, 77760 dofs
- Total Lagrangian form, finite strain, StVK [4]
- St. Venant-Kirchhoff material
- Sparse Cholesky linear solver (CHOLMOD[5])
- Newton-Raphson nonlinear solver
- Minimum compliance optimization problem

$$\begin{aligned} \underset{\mathbf{u}\in\mathbb{R}^{n_\mathbf{u}},\ \boldsymbol{\mu}\in\mathbb{R}^{n_{\boldsymbol{\mu}}}}{\text{minimize}} \quad & \mathbf{f_{ext}}^T\mathbf{u} \\ \text{subject to} \quad & V(\boldsymbol{\mu}) \leq \frac{1}{2}V_0 \\ & \mathbf{r}(\mathbf{u},\ \boldsymbol{\mu}) = 0 \end{aligned}$$

- Gradient computations: Adjoint method
- Optimizer: SNOPT [Gill et al., 2002]
- Maximum ROM size: $k_\mathbf{u} \leq 5$

[4] [Bonet and Wood, 1997, Belytschko et al., 2000]
[5] [Chen et al., 2008]

Optimal Solution Comparison

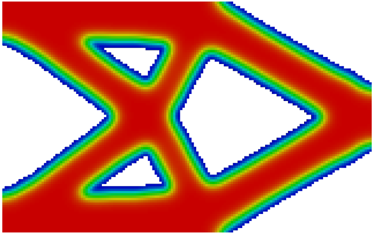

HDM

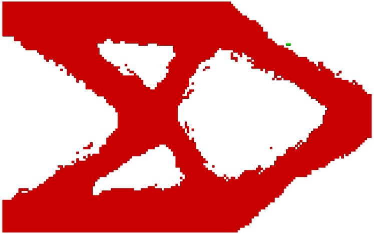

CTRPOD + $\boldsymbol{\Phi}_\mu$ adaptivity

HDM Solution	**HDM** Gradient	**HDM** Optimization
7458s (450)	4018s (411)	8284s

HDM
Elapsed time = 19761s

HDM Solution	**HDM** Gradient	**ROB** Construction	**ROM** Optimization
1049s (64)	88s (9)	727s (56)	39s (3676)

CTRPOD + $\boldsymbol{\Phi}_\mu$ adaptivity
Elapsed time = 2197s, Speedup ≈ 9x

Solution after 64 HDM Evaluations

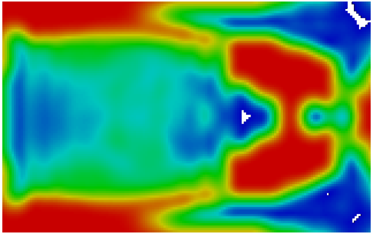

HDM

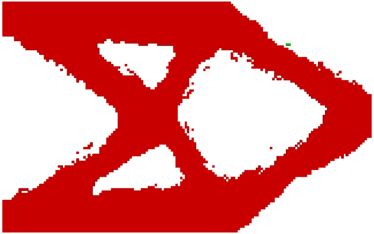

CTRPOD + Φ_μ adaptivity

- CTRPOD + Φ_μ adaptivity: superior approximation to optimal solution than HDM approach after fixed number of HDM solves (64)
- Reasonable option to *warm-start* HDM topology optimization

Macro-element Evolution

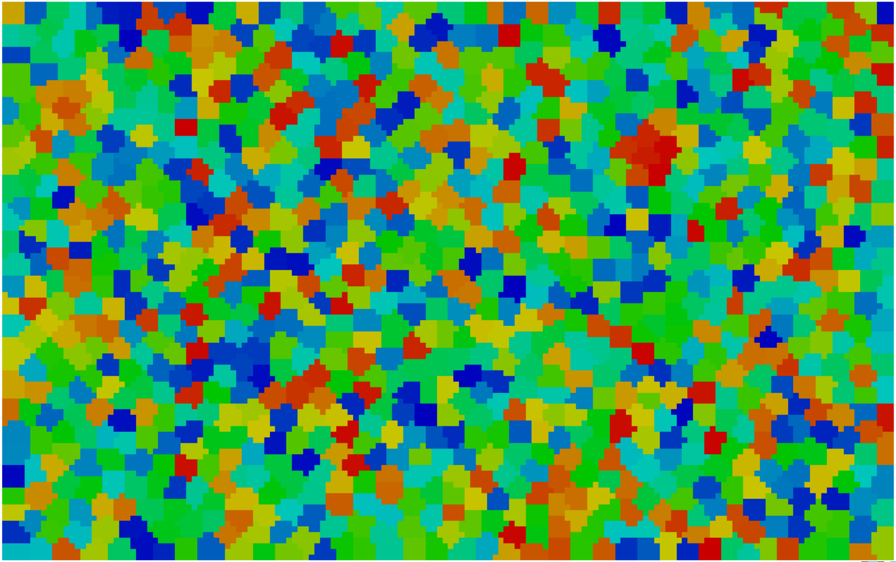

Iteration 0 (1000)

Macro-element Evolution

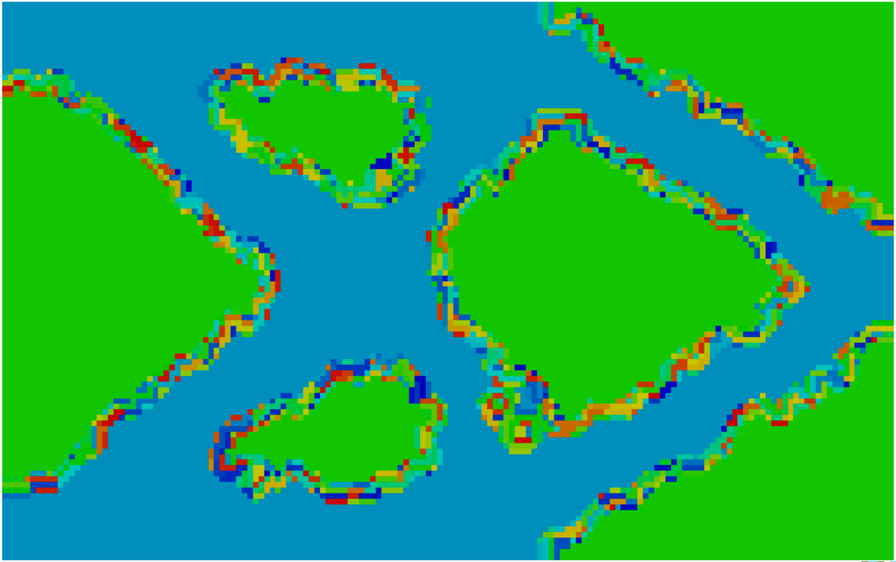

Iteration 1 (977)

Macro-element Evolution

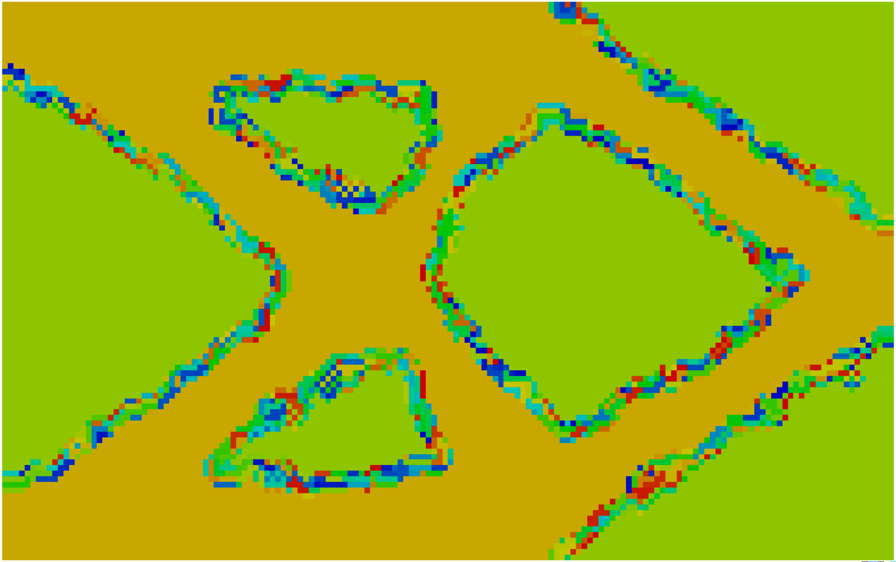

Iteration 2 (935)

Macro-element Evolution

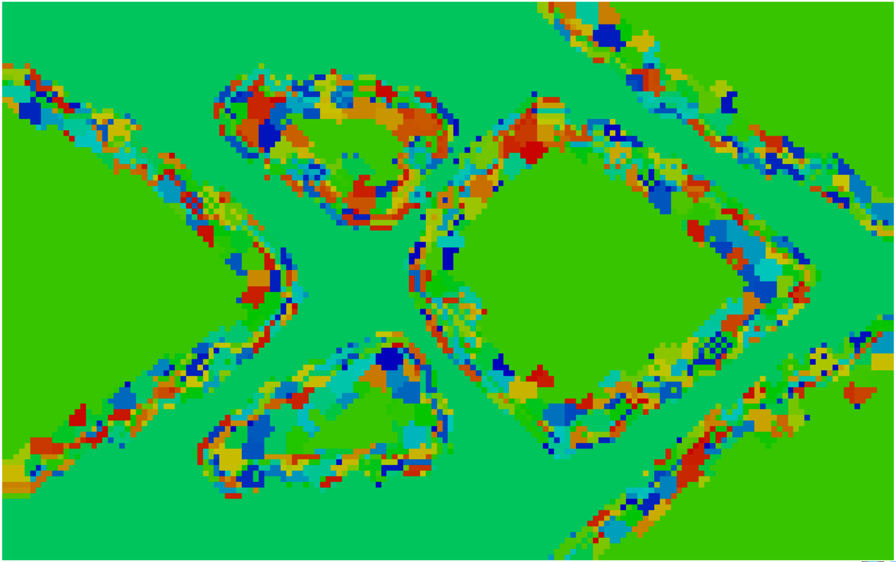

Iteration 3 (1152)

CTRPOD + Φ_μ adaptivity

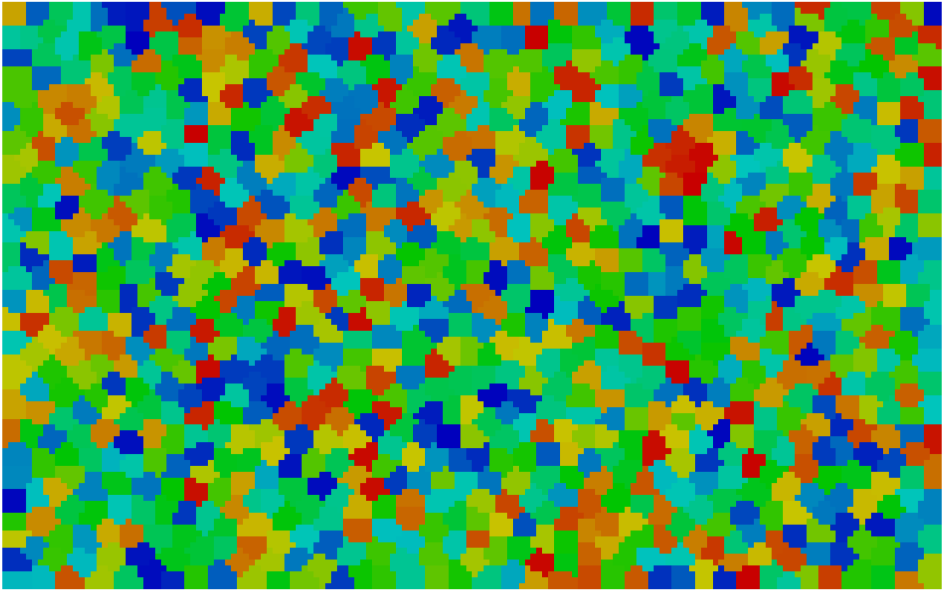

Problem Setup

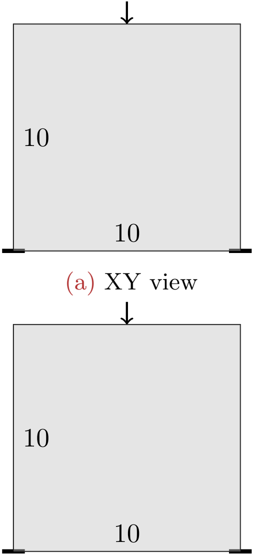

(a) XY view

(b) XZ view

- 64000 8-node brick elements, 206715 dofs
- Total Lagrangian formulation, finite strain
- St. Venant-Kirchhoff material
- Jacobi-Preconditioned Conjugate Gradient
- Newton-Raphson nonlinear solver
- Minimum compliance optimization problem

$$\begin{aligned} \underset{\mathbf{u}\in\mathbb{R}^{n_{\mathbf{u}}},\ \boldsymbol{\mu}\in\mathbb{R}^{n_{\boldsymbol{\mu}}}}{\text{minimize}} \quad & \mathbf{f}_{\text{ext}}{}^T\mathbf{u} \\ \text{subject to} \quad & V(\boldsymbol{\mu}) \leq 0.15\cdot V_0 \\ & \mathbf{r}(\mathbf{u},\ \boldsymbol{\mu}) = 0 \end{aligned}$$

- Gradient computations: Adjoint method
- Optimizer: SNOPT
- Maximum ROM size: $k_{\mathbf{u}} \leq 5$

Optimal Solution Comparison

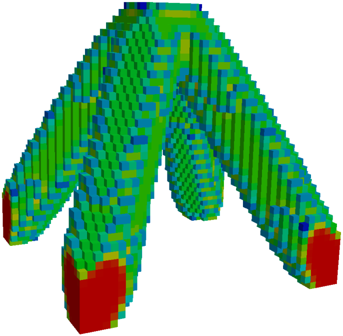

HDM

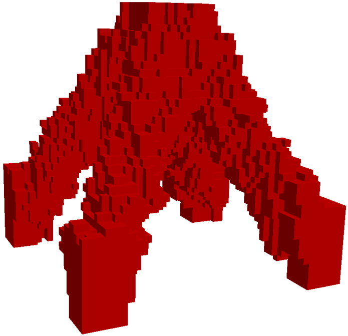

CTRPOD + Φ_μ adaptivity

- **HDM**, elapsed time = 179176s
- **CTRPOD**+Φ_μ adaptivity, elapsed time = 15208s
- Speedup $\approx 12\times$

Solution after 68 HDM Evaluations

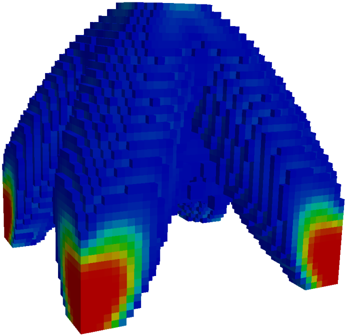

HDM

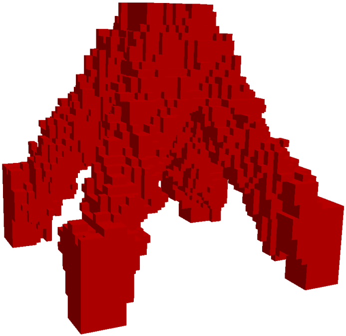

CTRPOD + Φ_μ adaptivity

- CTRPOD + Φ_μ adaptivity: superior approximation to optimal solution than HDM approach after fixed number of HDM solves (68)
- Reasonable option to *warm-start* HDM topology optimization

Summary and Future Work

Summary

- Framework introduced for accelerating PDE-constrained optimization problem with **side constraints** and **large-dimensional parameter space**
- Speedup attained via adaptive reduction of state space and parameter space
- Concepts/techniques borrowed from FEA and optimization theory
  - Dual-weighted residual error estimates
  - Theory of constrained optimization: Lagrangian, KKT system
- Applied to nonlinear topology optimization

Future Work

- Incorporation of error surrogates (ROMES) [Drohmann and Carlberg, 2014]
- Add fidelity to ROM using AMR instead of HDM solve [Carlberg, 2014]
- Incorporation of more sophisticated nonlinear model reduction methods to avoid $\mathcal{O}(k_{\mathbf{u}}^4 \cdot k_{\boldsymbol{\mu}})$ ROM cost
- Extension to unsteady PDE-constrained optimization [Zahr, Persson]
- Extension to stochastic PDE-constrained optimization [Zahr, Carlberg]

Contributions

- (MJZ) First work to define a **framework** for incorporating projection-based **reduced-order models** in **topology optimization** setting
  - Built on element volume fraction topology optimization formulation
  - Condition on $\boldsymbol{\Phi}_{\boldsymbol{\mu}}$ to enable use of SIMP (binary solutions) in reduced optimization problems
  - HDM Lagrange multiplier estimates from ROM Lagrange multipliers
- (MJZ) Generalization of TRPOD to work with constraints, i.e. CTRPOD
- (MJZ) Use of constrained optimization theory (KKT system) to *update/modify* parameter basis, $\boldsymbol{\Phi}_{\boldsymbol{\mu}}$
- (KW, MJZ) Practical details of framework
  - Local minima avoidance
  - Macroelement refinement
- (MJZ) Implementation: *pyMORTestbed* (C++/Python)
  - 3D FEM, topology optimization, model reduction

References I

Arian, E., Fahl, M., and Sachs, E. W. (2000).
Trust-region proper orthogonal decomposition for flow control.
Technical report, DTIC Document.

Barbič, J. and James, D. (2007).
Time-critical distributed contact for 6-dof haptic rendering of adaptively sampled reduced deformable models.
In *Proceedings of the 2007 ACM SIGGRAPH/Eurographics symposium on Computer animation*, pages 171–180. Eurographics Association.

Barrault, M., Maday, Y., Nguyen, N. C., and Patera, A. T. (2004).
An empirical interpolation method: application to efficient reduced-basis discretization of partial differential equations.
Comptes Rendus Mathematique, 339(9):667–672.

Belytschko, T., Liu, W., Moran, B., et al. (2000).
Nonlinear finite elements for continua and structures, volume 26.
Wiley New York.

Bonet, J. and Wood, R. (1997).
Nonlinear continuum mechanics for finite element analysis.
Cambridge university press.

References II

Carlberg, K. (2014).
Adaptive h-refinement for reduced-order models.
arXiv preprint arXiv:1404.0442.

Carlberg, K., Bou-Mosleh, C., and Farhat, C. (2011).
Efficient non-linear model reduction via a least-squares petrov–galerkin projection and compressive tensor approximations.
International Journal for Numerical Methods in Engineering, 86(2):155–181.

Chapman, T., Collins, P., Avery, P., and Farhat, C. (2015).
Accelerated mesh sampling for model hyper reduction.
International Journal for Numerical Methods in Engineering.

Chaturantabut, S. and Sorensen, D. C. (2010).
Nonlinear model reduction via discrete empirical interpolation.
SIAM Journal on Scientific Computing, 32(5):2737–2764.

Chen, Y., Davis, T. A., Hager, W. W., and Rajamanickam, S. (2008).
Algorithm 887: Cholmod, supernodal sparse cholesky factorization and update/downdate.
ACM Transactions on Mathematical Software (TOMS), 35(3):22.

References III

Constantine, P. G., Dow, E., and Wang, Q. (2014).
Active subspace methods in theory and practice: Applications to kriging surfaces.
SIAM Journal on Scientific Computing, 36(4):A1500–A1524.

Drohmann, M. and Carlberg, K. (2014).
The romes method for statistical modeling of reduced-order-model error.
SIAM Journal on Uncertainty Quantification.

Gill, P. E., Murray, W., and Saunders, M. A. (2002).
Snopt: An sqp algorithm for large-scale constrained optimization.
SIAM journal on optimization, 12(4):979–1006.

Holmes, P., Lumley, J. L., and Berkooz, G. (1998).
Turbulence, coherent structures, dynamical systems and symmetry.
Cambridge university press.

Lawson, C. L. and Hanson, R. J. (1974).
Solving least squares problems, volume 161.
SIAM.

References IV

Lieberman, C., Willcox, K., and Ghattas, O. (2010).
Parameter and state model reduction for large-scale statistical inverse problems.
SIAM Journal on Scientific Computing, 32(5):2523–2542.

Maute, K. and Ramm, E. (1995).
Adaptive topology optimization.
Structural optimization, 10(2):100–112.

Nguyen, N. and Peraire, J. (2008).
An efficient reduced-order modeling approach for non-linear parametrized partial differential equations.
International journal for numerical methods in engineering, 76(1):27–55.

Nocedal, J. and Wright, S. (2006).
Numerical optimization, series in operations research and financial engineering.
Springer.

Persson, P.-O., Willis, D., and Peraire, J. (2012).
Numerical simulation of flapping wings using a panel method and a high-order navier–stokes solver.
International Journal for Numerical Methods in Engineering, 89(10):1296–1316.

References V

Rewienski, M. J. (2003).
A trajectory piecewise-linear approach to model order reduction of nonlinear dynamical systems.
PhD thesis, Citeseer.

Sirovich, L. (1987).
Turbulence and the dynamics of coherent structures. i-coherent structures. ii-symmetries and transformations. iii-dynamics and scaling.
Quarterly of applied mathematics, 45:561–571.

PDE-Constrained Optimization: CFD Shape Optimization [6]

- Biologically-inspired flight
  - Micro aerial vehicles
- Mesh
  - 43,000 vertices
  - 231,000 tetra ($p = 3$)
  - 2,310,000 DOF
- CFD
  - Compressible Navier-Stokes
  - Discontinuous Galerkin
- Desired: shape optimization, control
  - unsteady effects
  - maximize thrust

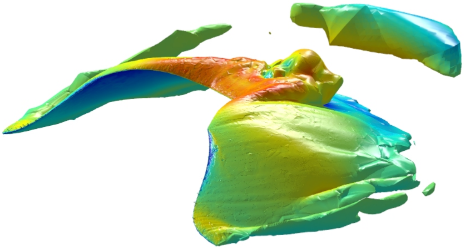

Figure: Flapping Wing [Persson et al., 2012]

[6] Current collaboration underway with P.-O. Persson to apply techniques outlined in this presentation to accelerate *unsteady* CFD shape optimization problems (3DG).

PDE-Constrained Optimization: CFD Shape Optimization

- Benchmark in automotive industry
- Mesh
  - 2,890,434 vertices
  - 17,017,090 tetra
  - 17,342,604 DOF
- CFD
  - Compressible Navier-Stokes
  - DES + Wall func
- Single forward simulation
  - $\approx$ 0.5 day on 512 cores
- Desired: shape optimization
  - unsteady effects
  - minimize average drag

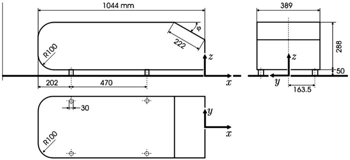

(a) Ahmed Body: Geometry (Ahmed et al, 1984)

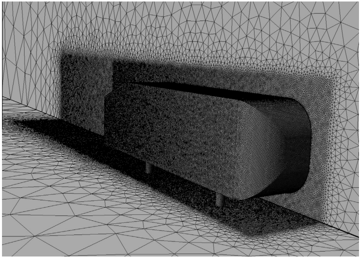

(b) Ahmed Body: Mesh (Carlberg et al, 2011)

Efficient Evaluation of Nonlinear Terms

- Due to the mixing of high-dimensional and low-dimensional terms in the ROM expression, only limited speedups available

$$\mathbf{r}_r(\mathbf{u}_r,\ \boldsymbol{\mu}_r) = \boldsymbol{\Phi}_{\mathbf{u}}{}^T \mathbf{r}(\boldsymbol{\Phi}_{\mathbf{u}}\mathbf{u}_r,\ \boldsymbol{\Phi}_{\boldsymbol{\mu}}\boldsymbol{\mu}_r) = 0$$

- To enable *pre-computation* of all large-dimensional quantities into low-dimensional ones, leverage *Taylor series expansion*

$$\begin{aligned}[\mathbf{r}_r(\mathbf{u}_r,\ \boldsymbol{\mu}_r)]_i = \mathbf{D}^0_{im}(\boldsymbol{\mu}_r)_m + \mathbf{D}^1_{ijm}(\mathbf{u}_r \times \boldsymbol{\mu}_r)_{jm} + \mathbf{D}^2_{ijkm}(\mathbf{u}_r \times \mathbf{u}_r \times \boldsymbol{\mu}_r)_{jkm} \\ + \mathbf{D}^3_{ijklm}(\mathbf{u}_r \times \mathbf{u}_r \times \mathbf{u}_r \times \boldsymbol{\mu}_r)_{jklm} = 0\end{aligned}$$

where

$$\mathbf{D}^3_{ijklm} = \frac{\partial^3 \mathbf{r}_t}{\partial \mathbf{u}_p \partial \mathbf{u}_q \partial \mathbf{u}_s}(\hat{\mathbf{u}},\ \boldsymbol{\phi}^m_{\boldsymbol{\mu}})(\boldsymbol{\phi}^i_{\mathbf{u}} \times \boldsymbol{\phi}^j_{\mathbf{u}} \times \boldsymbol{\phi}^k_{\mathbf{u}} \times \boldsymbol{\phi}^l_{\mathbf{u}})_{tpqs}$$

- Related work: [Rewienski, 2003, Barrault et al., 2004, Barbič and James, 2007, Nguyen and Peraire, 2008, Chaturantabut and Sorensen, 2010, Carlberg et al., 2011]

Offline/Online Decomposition for Optimization

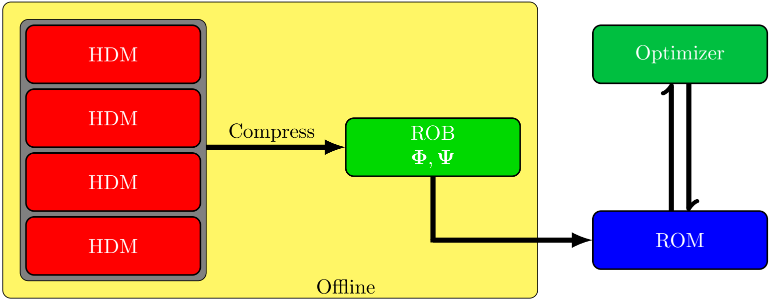

(a) Schematic of Offline/Online Decomposition for ROM Optimization

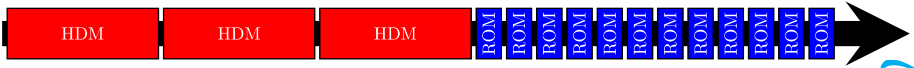

(b) Breakdown of Computational Effort

Offline/Online Decomposition for ROM Optimization

(a) Idealized Optimization Trajectory: Parameter Space

Offline/Online Decomposition for ROM Optimization

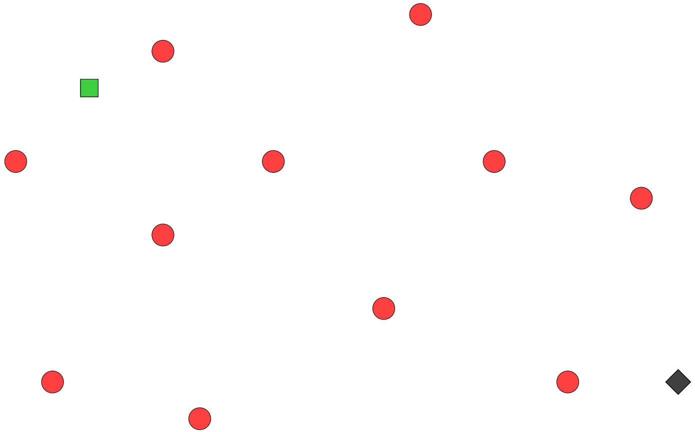

(a) Idealized Optimization Trajectory: Parameter Space

Offline/Online Decomposition for ROM Optimization

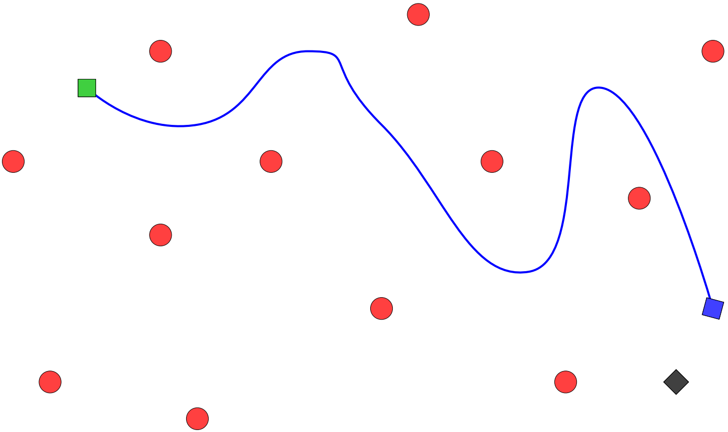

(a) Idealized Optimization Trajectory: Parameter Space

Problem Setup

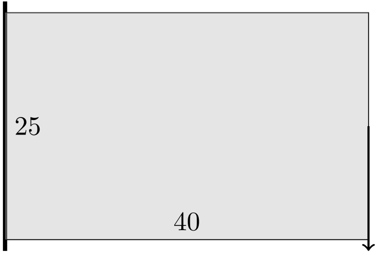

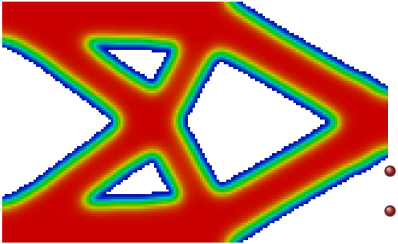

- 16000 8-node brick elements, 77760 dofs
- Total Lagrangian form, finite strain, StVK [7]
- St. Venant-Kirchhoff material
- Sparse Cholesky linear solver (CHOLMOD[8])
- Newton-Raphson nonlinear solver
- Minimum compliance optimization problem

$$\begin{aligned} \underset{\mathbf{u}\in\mathbb{R}^{n_\mathbf{u}},\ \boldsymbol{\mu}\in\mathbb{R}^{n_{\boldsymbol{\mu}}}}{\text{minimize}} \quad & \mathbf{f}_{\text{ext}}{}^T\mathbf{u} \\ \text{subject to} \quad & V(\boldsymbol{\mu}) \leq \frac{1}{2}V_0 \\ & \mathbf{r}(\mathbf{u},\ \boldsymbol{\mu}) = 0 \end{aligned}$$

- Gradient computations: Adjoint method
- Optimizer: SNOPT [Gill et al., 2002]

[7] [Bonet and Wood, 1997, Belytschko et al., 2000]
[8] [Chen et al., 2008]

Numerical Experiment: Offline-Online

- Parameter reduction ($\boldsymbol{\Phi}_{\boldsymbol{\mu}}$)
  - *apriori spatial clustering*
  - $k_{\boldsymbol{\mu}} = 200$
- *Greedy* Training
  - 5000 candidate points (LHS)
  - 50 snapshots
  - Error indicator: $||\mathbf{r}(\boldsymbol{\Phi}_{\mathbf{u}}\mathbf{u}_r, \ \boldsymbol{\Phi}_{\boldsymbol{\mu}}\boldsymbol{\mu}_r)||$
- State reduction ($\boldsymbol{\Phi}_{\mathbf{u}}$)
  - POD
  - $k_{\mathbf{u}} = 25$
  - Polynomialization acceleration

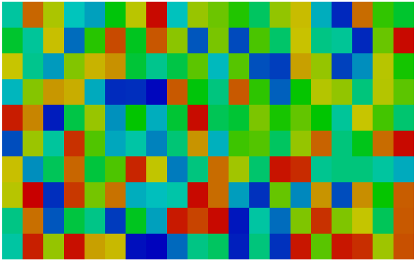

Material Basis

Numerical Experiment: Offline-Online

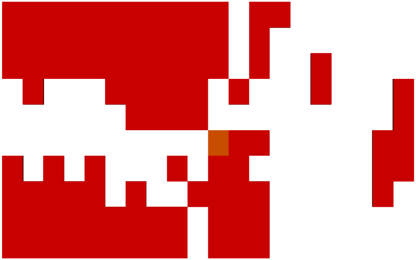

Optimal Solution (ROM)

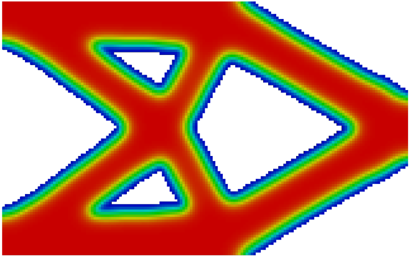

Optimal Solution (HDM)

HDM Solution	**ROB** Construction	**Greedy** Algorithm	**ROM** Optimization
2.84×10^3 s	5.48×10^4 s	1.67×10^5 s	30 s
1.26%	24.36%	74.37%	0.01%

HDM Optimization: 1.97×10^4 s

Lagrange Multiplier Estimate

Lagrange Multiplier, Constraint Pairs

$\boldsymbol{\lambda}$	$\boldsymbol{\lambda}_r$	$\boldsymbol{\tau}$	$\boldsymbol{\tau}_r$
$\mathbf{c}(\mathbf{u},\ \boldsymbol{\mu}) \geq 0$	$\mathbf{c}(\boldsymbol{\Phi}_\mathbf{u}\mathbf{u}_r,\ \boldsymbol{\Phi}_\boldsymbol{\mu}\boldsymbol{\mu}) \geq 0$	$\mathbf{A}\boldsymbol{\mu} \geq \mathbf{b}$	$\mathbf{A}_r\boldsymbol{\mu}_r \geq \mathbf{b}_r$

Goal: Given $\mathbf{u}_r,\ \boldsymbol{\mu}_r,\ \boldsymbol{\tau}_r \geq 0,\ \boldsymbol{\lambda}_r \geq 0$, estimate $\tilde{\boldsymbol{\tau}} \geq 0,\ \tilde{\boldsymbol{\lambda}} \geq 0$ to compute

$$\nabla_\boldsymbol{\mu}\mathcal{L}(\boldsymbol{\Phi}_\boldsymbol{\mu}\boldsymbol{\mu}_r,\ \tilde{\boldsymbol{\lambda}},\ \tilde{\boldsymbol{\tau}}) = \frac{\partial \mathcal{J}}{\partial \boldsymbol{\mu}}(\boldsymbol{\Phi}_\mathbf{u}\mathbf{u}_r,\ \boldsymbol{\Phi}_\boldsymbol{\mu}\boldsymbol{\mu}_r) - \frac{\partial \mathbf{c}}{\partial \boldsymbol{\mu}}(\boldsymbol{\Phi}_\mathbf{u}\mathbf{u}_r,\ \boldsymbol{\Phi}_\boldsymbol{\mu}\boldsymbol{\mu}_r)^T\tilde{\boldsymbol{\lambda}} - \mathbf{A}^T\tilde{\boldsymbol{\tau}}$$

Lagrange Multiplier Estimates

$$\tilde{\boldsymbol{\lambda}} = \boldsymbol{\lambda}_r$$

$$\tilde{\boldsymbol{\tau}} = \underset{\boldsymbol{\tau}\geq 0}{\arg\min} \left|\left|\mathbf{A}^T\boldsymbol{\tau} - \left(\frac{\partial \mathcal{J}}{\partial \boldsymbol{\mu}}(\boldsymbol{\Phi}_\mathbf{u}\mathbf{u}_r,\ \boldsymbol{\Phi}_\boldsymbol{\mu}\boldsymbol{\mu}_r) - \frac{\partial \mathbf{c}}{\partial \boldsymbol{\mu}}(\boldsymbol{\Phi}_\mathbf{u}\mathbf{u}_r,\ \boldsymbol{\Phi}_\boldsymbol{\mu}\boldsymbol{\mu}_r)^T\tilde{\boldsymbol{\lambda}}\right)\right|\right|$$

Non-negative least squares: [Lawson and Hanson, 1974, Chapman et al., 2015]

Standard Difficulty: Checkerboarding

Gradient Filtering, Nodal Projection

- Minimum length scale, r_{min}
- Gradient Filtering [9]

$$\widehat{\frac{\partial \mathcal{J}}{\partial \boldsymbol{\mu}_k}} = \frac{\sum_{j \in S_k} H_{kj} \boldsymbol{\mu}_i \frac{\partial \mathcal{J}}{\partial \boldsymbol{\mu}_i}}{\boldsymbol{\mu}_k \sum_{j \in S_k} H_{kj}}$$

- Nodal Projection

$$\boldsymbol{\mu}_k = \frac{\sum_{j \in \mathcal{S}_k} \boldsymbol{\tau}_j H_{jk}}{\sum_{j \in \mathcal{S}_k} H_{jk}}$$

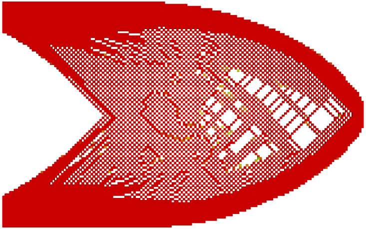

(a) Without projection/filtering

[9] $H_{ki} = r_{\text{min}} - \text{dist}(k,\ i)$

Standard Difficulty: Checkerboarding

Gradient Filtering, Nodal Projection

- Minimum length scale, $r_{\min}$
- Gradient Filtering [9]

$$\frac{\widehat{\partial \mathcal{J}}}{\partial \boldsymbol{\mu}_k} = \frac{\sum_{j \in S_k} H_{kj} \boldsymbol{\mu}_i \frac{\partial \mathcal{J}}{\partial \boldsymbol{\mu}_i}}{\boldsymbol{\mu}_k \sum_{j \in S_k} H_{kj}}$$

- Nodal Projection

$$\boldsymbol{\mu}_k = \frac{\sum_{j \in \mathcal{S}_k} \boldsymbol{\tau}_j H_{jk}}{\sum_{j \in \mathcal{S}_k} H_{jk}}$$

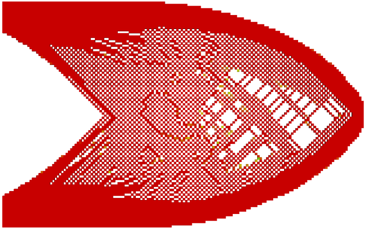

(a) Without projection/filtering

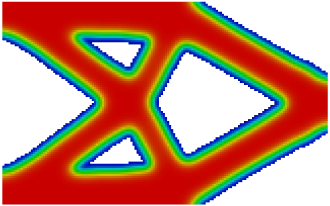

(b) With projection

[9] $H_{ki} = r_{\min} - \operatorname{dist}(k, i)$

Standard Difficulty: Checkerboarding

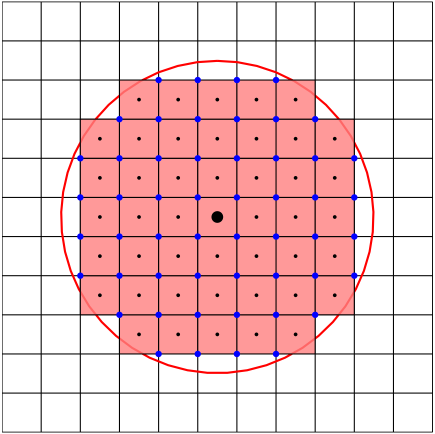

Standard Difficulty: Checkerboarding

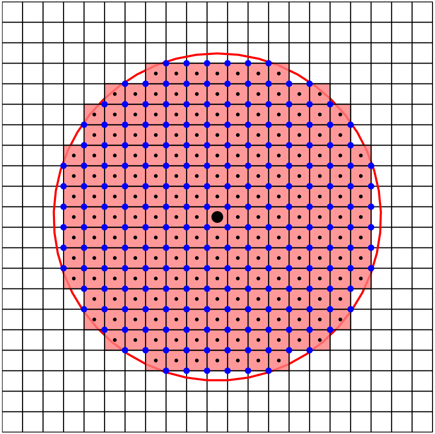

Standard Difficulty: Checkerboarding

Implication for ROM

- Nonlocal introduced through projection/filtering
- μ_e influences volume fraction of all elements within $r_{\min}$ of element/node e
- Clashes with requirement on Φ_μ of columns with non-overlapping non-zeros
- Handled heuristically by performing parameter basis adaptation to eliminate "checkerboard" regions of parameter space, uses concept of $r_{\min}$

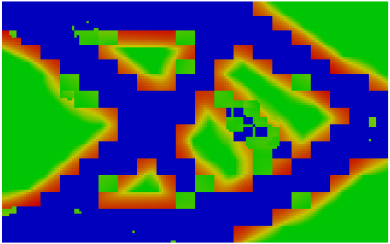

Gradient of Lagrangian

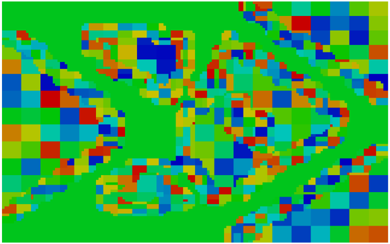

Updated Macroelements